molecular pharmaceutics

Article

pubs.acs.org/molecularpharmaceutics

Quantitative Detection of PLGA Nanoparticle Degradation in Tissues following Intravenous Administration

Abdul Khader Mohammad and Joshua J. Reineke*

Department of Pharmaceutical Sciences, Eugene Applebaum College of Pharmacy and Health Sciences, Wayne State University, Detroit, Michigan 48201, United States

Supporting Information

ABSTRACT: The biodegradable polymer poly(lactic-*co*-glycolic) acid (PLGA) has been extensively utilized and investigated as a drug delivery system. Although *in vivo* biodegradation (at specific administration sites only) of PLGA-based drug delivery constructs, such as foams and microparticles, has been studied, quantitative *in vivo* biodegradation of distributed polymer nanoparticles has not been accomplished and is quintessential for designing formulations to achieve desired pharmacokinetic properties of a drug in a target tissue. We determined the *in vivo* degradation kinetics of PLGA nanoparticles, of two sizes, distributed in liver, spleen, and lungs following intravenous administration. In addition, we simultaneously determined the amount of polymer in tissues. Nanoparticle degradation *in vitro* and *in vivo* appears to be a first-order process, and useful correlations were obtained between *in vitro* and *in vivo* tissue degradation of the nanoparticles. The ability to detect *in vivo* degradation and biodistribution of polymer nanoparticles is a significant milestone for the rational design of degradable nanoparticle-based drug delivery systems capable of delivering the therapeutic agent in a closely predictable manner to target tissue.

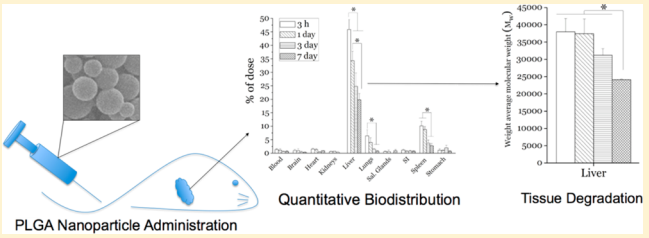

KEYWORDS: *biodegradation, degradation, biodistribution, drug delivery, liver*

1. INTRODUCTION

Nanoparticle delivery systems have tremendous potential in clinical applications, and there are already several successful nanoparticle systems in use for various diseases.[1] The *in vitro* degradation of poly(lactic-*co*-glycolic) acid (PLGA) microparticles and nanoparticles has been investigated from quantitative as well as qualitative standpoints.[2−4] *In vivo* degradation of PLGA-based drug delivery constructs, such as foams, scaffolds, stents, films, and microparticles (ectopic), has been studied by direct implantation of these structures.[5,6] However, to the best of our knowledge, no previous reports have quantitatively examined the *in vivo* degradation of biodegradable microparticles or nanoparticles in tissues after systemic administration, i.e., as distributed nano/microparticles. This lack of quantitative information on *in vivo* degradation kinetics, an important parameter that controls drug release, makes it difficult to design optimal drug delivery systems with predictable drug release properties in target tissues. Further, a better understanding of *in vivo* nanoparticle dynamics, including degradation, could lead to more predictable organ distribution profiles.

Conventionally, drug release from PLGA nanoparticles *in vitro* is used to predict release *in vivo*. However, *in vitro* drug release might not be the same as that *in vivo* particularly when release is degradation dependent. Even from a theoretical perspective, the expected *in vivo* degradation is difficult to postulate. For instance, the role of enzymes in PLGA degradation is still debated.[7−9] Given that nanoparticle degradation plays a crucial role in sustained drug release[10] and may play an equally crucial role in biodistribution (as we discussed in a recent review[11]), we aimed to measure quantitatively the *in vivo* degradation of PLGA nanoparticles after intravenous administration.

We investigated the *in vivo* biodegradation of PLGA nanoparticles of mean sizes 215 ± 18 nm and 501 ± 31 nm, hereafter referred to as 200 nm and 500 nm, respectively, after intravenous administration in tail vein of mice. After injection of nanoparticles, the tissues were extracted at 3 h, 1 day, 3 days, and 1 week. The degradation process, as measured by decrease in weight average molecular weight (M_w), occurs via ester bond scission in the polymer backbone, which releases the encapsulated drug from the nanoparticle. We found that *in vitro* degradation of nanoparticles of both sizes had a first-order degradation kinetic profile. The smaller, 200 nm nanoparticles had faster *in vivo* degradation in liver and spleen compared to *in vitro* degradation. The larger, 500 nm nanoparticles had relatively similar *in vivo* and *in vitro* degradation rates in the liver, but in the spleen the degradation rate was slower *in vivo*. The methodology utilized here to measure *in vivo* degradation

Special Issue: Emerging Technology in Evaluation of Nanomedicine

Received: October 1, 2012
Revised: March 19, 2013
Accepted: March 19, 2013
Published: March 19, 2013

and organ biodistribution of PLGA nanoparticles can be applied, either directly or with modification, to other degradable polymer systems, including polyanhydrides, polyamides, polyesters, poly(cyano acrylates), polyurethanes, poly orthoesters, polydihydropyrans, and polyacetals.

2. EXPERIMENTAL SECTION

2.1. Materials. PLGA (50:50) of molecular weight (M_w) 44,000 Da was provided by Purac Biomaterials (USA). Polyvinyl alcohol (PVA) of molecular weight 88,000 Da and phosphate-buffered saline (PBS; pH 7.4) were purchased from Fisher Scientific (USA). All organic solvents were purchased from Fisher Scientific and were of HPLC grade.

2.2. Fabrication of PLGA Nanoparticles. PLGA nanoparticles were fabricated by two different methods. For the 200 nm nanoparticles, a 0.9% w/v PLGA solution in acetone was added dropwise to an aqueous solution of 1% w/v PVA at a stirring speed of 800 rpm overnight.[12] The nanoparticles were centrifuged at 40000*g* for 1 h, washed with 30 mL of deionized water thrice, resuspended in 15 mL of deionized water, frozen, and lyophilized. For the 500 nm nanoparticles, we slightly modified a previous method.[13] Briefly, 2 mL of 5% w/v PLGA solution in dichloromethane was added to 30 mL of 0.5% w/v PVA and sonicated at 30 W for 10 min on an ice bath. This preparation was then added to 100 mL of deionized water under magnetic stirring at 600 rpm overnight. The preparation was centrifuged at 20000*g* to collect the nanoparticles, washed thrice in 30 mL of deionized water, resuspended in 15 mL of deionized water, frozen, and lyophilized.

2.3. Nanoparticle Characterization. Formulations were reconstituted with a 0.5% w/v PVA solution and sonicated for 30−60 s in a bath sonicator to make a 0.1% w/v nanoparticle suspension. The suspension was then subjected to size analysis by dynamic light scattering on a 90Plus Particle Size Analyzer (Brookhaven Instrument Corporation). The light scattering data provides the mean nanoparticle size as well as the nanoparticle polydispersity index (nPDI), which is defined as the square of the standard size deviation divided by the mean diameter. For scanning electron microscopy, a small amount of the lyophilized formulation was mounted on carbon adhesive tape and sputter-coated with gold using a 70 mA current for 30 s. Images of the formulation were captured at a working distance of 7 mm and an accelerating voltage of 25 kV with a Hitachi S-2400 scanning electron microscope.

2.4. *In Vitro* Degradation. For *in vitro* degradation, 10 mg of the PLGA nanoparticles was suspended in 1.25 mL of PBS and incubated at 37 °C on a mixer. The samples were removed from the incubator at predetermined time points and lyophilized. Dried samples were dissolved in chloroform and subjected to analysis by gel permeation chromatography (GPC) (GPC Max VE 2001, Viscotek Corporation) equipped with a column bank consisting of three columns with size exclusion limits of 4 million, 70,000, and 5,000 Da. A refractive index detector (VE 3580, Viscotek Corporation) was used to detect PLGA retention time. We used universal calibration to calculate the molecular weight of PLGA. In conjunction with the refractive index detector, a 4-bridge, viscometer (Viscotek Corporation) was used to yield inherent viscosity for universal calibration with a calibration curve of retention time versus log molecular weight of narrow standard polystyrene samples of molecular weights ranging from 1,000 to 90,000 Da. In addition to molecular weight information, GPC analysis also yields the polymer polydispersity index (pPDI), which is defined as the weight average molecular weight divided by the number average molecular weight. It should be noted that this is unrelated and differentiated from the nPDI defined in section 2.3.

2.5. Preparation of Nanoparticle Suspension and Intravenous Administration. The nanoparticles were suspended in sterilized 0.9% sodium chloride solution at a concentration of 3% w/v and sonicated in a water bath for 30 min. Before the nanoparticles were administered to each animal, the formulation was sonicated for 10 min. Degradation analysis yielded no degradation of nanoparticle formulations using this suspension protocol. Male Balb/c mice weighing 20−25 g (Charles River Inc.) were used after acclimation for a week. Food and water were available to the animals *ad libitum*.

The PLGA nanoparticles in suspension were administered to the mice via tail vein injection. Each animal received 300 μL of the nanoparticle suspension. For all study groups, $n = 3$. All animal procedures adhered to American Veterinarian Medical Association (AVMA) Guidelines, received Wayne State University Institutional Animal Care and Use Committee (IACUC) approval, were in accordance with the Office of Laboratory Animal Welfare (OLAW) Public Health Service Policy on Humane Care and Use of Laboratory Animals, and followed the NIH's "Principles of Laboratory Animal Care." Based on what is known from the literature about the hydrophobic nature and size of the unmodified PLGA nanoparticles, they were expected to distribute rapidly in relatively high amounts to the liver and spleen as a result of mononuclear phagocyte system sequestration.[14−16] These particles were chosen explicitly for this reason to ensure high tissue concentration of nanoparticles. Sensitivity of the analysis method for application to a diverse range of nanoparticle systems is currently being improved.

2.6. Tissue Harvesting and Sample Preparation. At 3 h and 1, 3, and 7 days after intravenous administration of nanoparticles, tissues including liver, spleen, kidneys, heart, brain, lungs, and lymph nodes (axillary, brachial, cervical, and mesenteric lymph nodes) were extracted, processed, and analyzed by a method similar to that described previously.[17] These time points were selected based on experimentally determined *in vitro* degradation rates and an expectation that *in vivo* degradation would proceed much faster. Briefly, the tissues were homogenized, lyophilized, and then mixed for 4 days with chloroform to extract polymer. The tissue mixture in chloroform was then filtered using positive pressure filtration, and the chloroform solution, containing polymer, was collected in a glass vial. This solution was frozen and lyophilized before GPC analysis.

2.7. Biodegradation and Biodistribution of Nanoparticles *in Vivo*. Analysis of polymer concentration and determination of molecular weight from tissue extracts was performed by GPC as described above for *in vitro* degradation (section 2.4). To determine the biodistribution of nanoparticles *in vivo*, the area under the curve for each sample was calculated by Omni SEC software, and the amount of nanoparticles in each tissue was calculated as a percentage of the administered dose. To ensure that any degradation observed was not a result of tissue processing, the PLGA nanoparticles were processed as described for the tissue extracts. No degradation was observed upon GPC analysis of the samples. To validate the method of tissue extraction, PLGA samples of known concentration and chromography profile (M_w) were used to dope blank tissue samples prior to processing. These doped samples were indistinguishable from the chromography profile of the starting

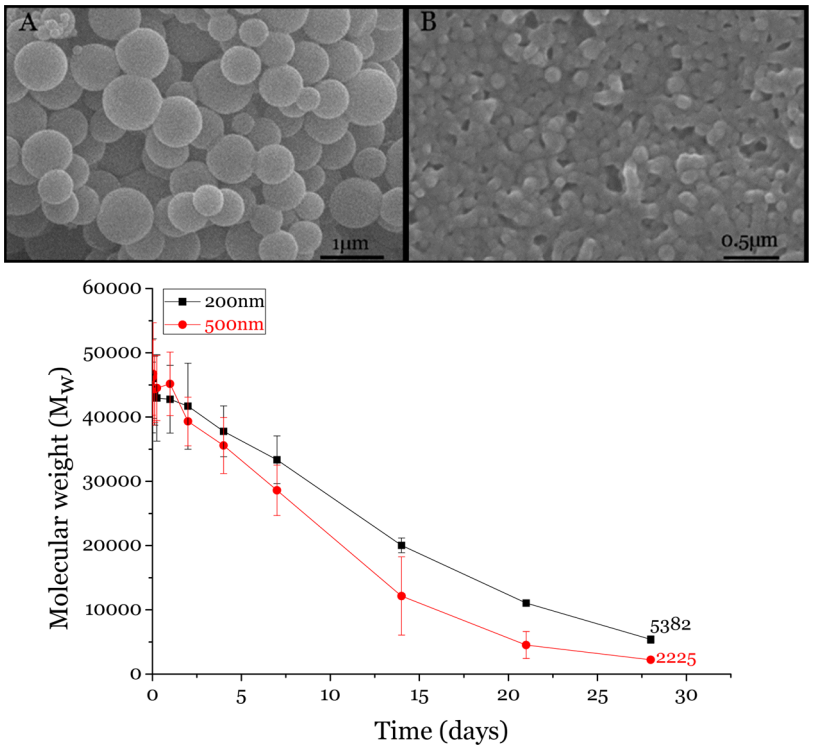

Figure 1. Scanning electron microscopic images of PLGA nanoparticles of size (a) 500 nm and (b) 200 nm. (c) *In vitro* degradation profile of PLGA nanoparticles.

material and resulted in a slight underestimate of the concentration (>97% of doped PLGA was detected in all samples). Glass transition (T_g) shift, as measured by differential scanning calorimetry (TA Instruments Q2000), was also used to confirm molecular weight change (data not shown). Although the differential scanning calorimetry and GPC results were consistent, T_g shifts were too subtle for direct quantitative correlation.

2.8. Statistical Analysis. Statistical analysis was performed using one-way ANOVA followed by Tukey's post hoc analysis where applicable, with OriginPro8 software.

3. RESULTS AND DISCUSSION

3.1. Nanoparticle Characteristics. Each nanoparticle formulation is monodisperse (215 ± 18 nm and 501 ± 31 nm; nPDI <0.1), and particles have a smooth surface (Figures 1a and 1b). From the *in vitro* degradation data, the 500 nm nanoparticles had a faster rate of degradation than the 200 nm nanoparticles (Figure 1c). A similar size-based difference in degradation rate was reported by Dunne and co-workers.[10] In the large nanoparticles, the degraded polymer fractions have a longer path to diffuse out of the particle interior to the surface resulting in accumulation of these oligomers. This local acidification, resulting from the trapped oligomers, leads to the autocatalysis of PLGA chains. Conversely, in smaller particles the degraded fractions diffuse out faster.[10]

3.2. Biodistribution of PLGA Nanoparticles following Intravenous Administration. For both sizes of nanoparticles, the liver was the site of highest deposition, followed by spleen and lungs (Figures 2 and 3). This result is in agreement with the fact that nanoparticles with hydrophobic surfaces are rapidly sequestered from the circulation by organs of the mononuclear phagocyte system.[18] The 500 nm nanoparticles deposit in the liver to a greater extent than the 200 nm nanoparticles. This is

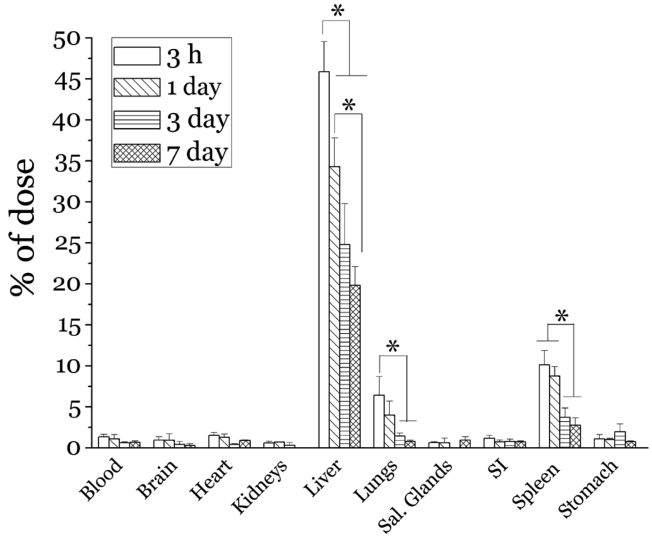

Figure 2. Biodistribution of PLGA nanoparticles 500 nm in diameter. *p < 0.05 (n = 3; mean ± SD).

also in agreement with the fact that the optimum size for phagocytic uptake is 250 nm to 3 μm.[19] Specifically, at 3 h the 500 nm PLGA nanoparticles had a higher deposition in liver, at 45.9% of the administered dose (Figure 2), whereas the 200 nm nanoparticles had a liver deposition rate of 32.3% (Figure 3). The greater deposition of larger nanoparticles in liver could be the result of more efficient uptake by Kupffer cells. In accordance with this observation, other reports have shown that larger nanoparticles have greater accumulation in the liver.[20] However, in the spleen, nanoparticles of both sizes had a similar deposition (10.1% and 10.5% of administered dose) at the end of 3 h (Figures 2 and 3). The amount of nanoparticles

dx.doi.org/10.1021/mp300559v | *Mol. Pharmaceutics* 2013, 10, 2183−2189

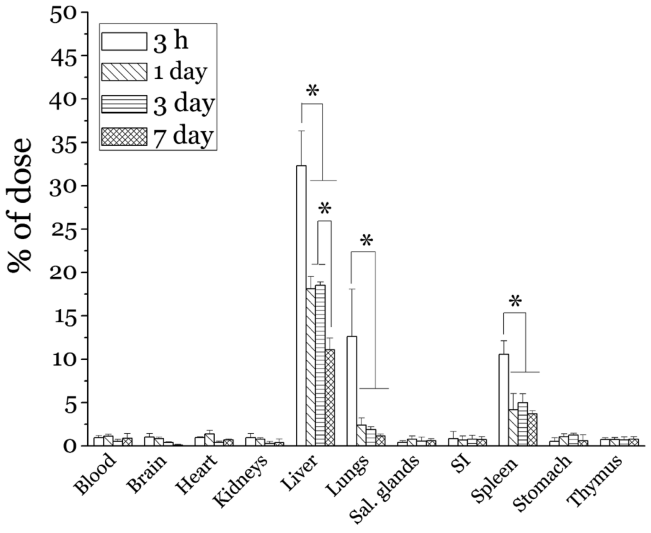

Figure 3. Biodistribution of PLGA nanoparticles 200 nm in diameter. *$p < 0.05$ ($n = 3$; mean ± SD).

in these tissues decreased with time, likely as a result of degradation and subsequent removal of the soluble oligomers/monomers from the organs in addition to possible redistribution of nanoparticles to other tissues. The decrease in the amount of nanoparticles over time and the overall loss of mass in all tissues combined are shown in Figure 4.

3.3. *In Vivo* Biodegradation of PLGA Nanoparticles following Intravenous Administration. For both nanoparticle sizes, because the liver was the site of highest nanoparticle deposition, followed by spleen, we determined the degradation of nanoparticles in these two tissues. Data on the weight-average molecular weight (M_w) for each condition are presented in bar graphs for ease of comparison (Figures 5 and 6). However, the full data set is also presented in Supplementary Table 1 in the Supporting Information along with a representative chromatograph overlay of 200 nm nanoparticle tissue degradation at 1 and 7 days in the liver (Supplemental Figure 1 in the Supporting Information). In the two tissues studied, degradation in the liver was highest (Figures 5 and 6). For the 500 nm nanoparticles, the M_w at 3 h and 24 h was 36,879 Da and 40,427 Da, respectively. The M_w decreased to 31,377 Da by 72 h and to 23,623 Da at the end of 1 week. In the spleen, at the end of 3 h and 24 h, the M_w was 39,557 Da and 38,111 Da, respectively. It decreased to 35,076 Da by 72 h and to 28,153 Da at the end of 1 week. The degradation process seems to have a lag phase (i.e., little degradation) up to at least 24 h, after which we see a greater decrease in M_w by 72 h. For the 200 nm nanoparticles, extensive degradation was observed in the liver. The M_w at the end of 3 h and 24 h was 37,970 Da and 37,417 Da, respectively. Thereafter, it decreased to 31,192 Da by 72 h and 24,116 Da at the end of 1 week. In spleen, the M_w at the end of 3 h and 24 h was 38,449 Da and 39,704 Da, respectively; by 72 h the M_w decreased to 31,633 Da and then to 25,550 Da at the end of 1 week (Figure 6).

Degradation *in vitro* was faster in the 500 nm nanoparticles than the 200 nm nanoparticles (Figure 1c) as discussed in section 3.1. However, in the liver there was little difference in the extent of degradation between the two particle sizes. At the end of 1 week, the M_w for 500 nm and 200 nm nanoparticles was 23,623 Da and 24,116 Da, respectively. In the spleen, at 3 h

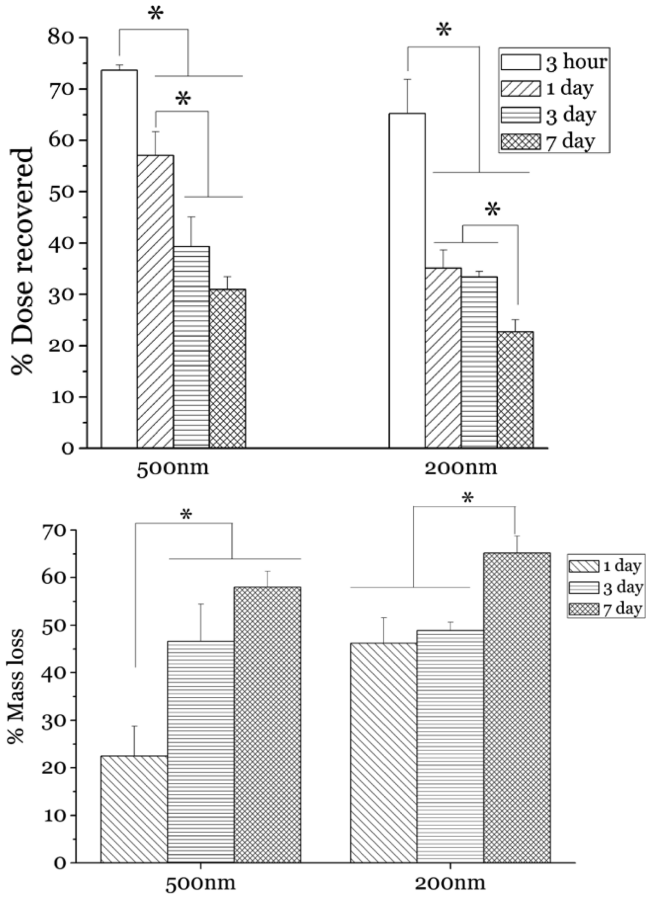

Figure 4. (a, top) Total amount of nanoparticles detected from all tissues represented as the percentage of the administered dose recovered. (b, bottom) Percent decrease in the total amount of nanoparticles detected from all the tissues at three time points (1, 3, and 7 days) relative to the amount deposited at 3 h. *$p < 0.05$ ($n = 3$; mean ± SD).

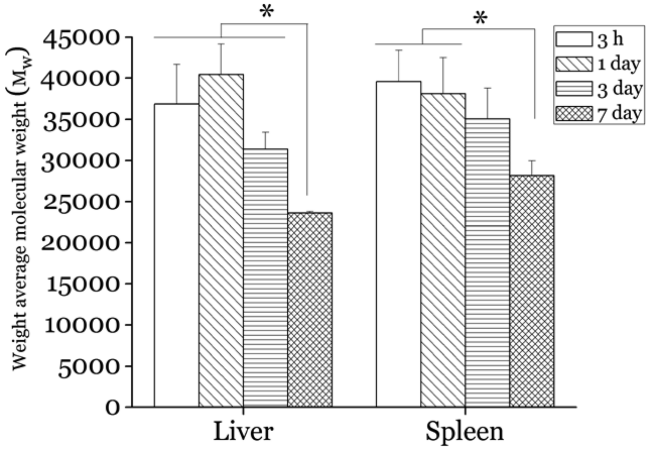

Figure 5. The biodegradation of PLGA nanoparticles 500 nm in diameter. *$p < 0.05$ ($n = 3$; mean ± SD).

and 24 h there was little difference in the M_w between both nanoparticle sizes. At 3 h, the M_w for 500 nm and 200 nm nanoparticles was 39,557 Da and 38,449 Da, respectively. In spleen, at the end of 24 h the M_w was 38,111 Da and 39,704 Da for 500 nm and 200 nm size nanoparticles, respectively. At the end of 3 days, the M_w was 35,076 Da and 31,633 Da for 500 nm

dx.doi.org/10.1021/mp300559v | *Mol. Pharmaceutics* 2013, 10, 2183−2189

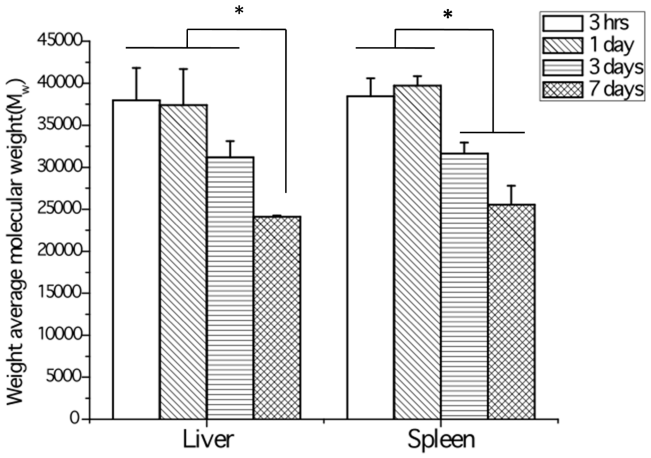

Figure 6. The biodegradation of PLGA nanoparticles 200 nm in diameter. *$p < 0.05$ ($n = 3$; mean ± SD).

and 200 nm nanoparticles, respectively. At the end of 1 week, the M_w degraded further to 28,153 Da and 25,550 Da in 500 nm and 200 nm nanoparticles, respectively (Figures 5 and 6).

Furthermore, the 500 nm nanoparticles had greater deposition in the liver, but *in vivo* degradation was similar to that of the 200 nm nanoparticles. In the liver, compared to the M_w at 3 h, the 500 nm nanoparticles had a 35.9% reduction in M_w, and the 200 nm nanoparticles had a 36.4% reduction in M_w at the end of 1 week. In spleen, relative to the M_w at 3 h, the 500 nm nanoparticles had a 28.8% reduction in M_w, whereas the 200 nm nanoparticles had a decrease of 33.5% at the end of 1 week. Despite the similar reduction in polymer molecular weights in both the tissues, it must be kept in mind that the liver had much higher nanoparticle deposition; therefore, the total degradation in liver is much higher than that in spleen. Additionally, the higher level of nanoparticle degradation in the liver over other tissues might be attributed to the presence of several esterases that have higher concentrations in the liver.[21] Therefore, we believe, as a result of differences in enzymes in these different tissues, that the degree of degradation varies in these tissues, with liver being the tissue with the highest nanoparticle biodegradation and esterase concentrations. However, one limitation of this study is that the nanoparticle location at the level of cell type or cellular compartment is not known. Such factors might also greatly affect degradation. Nevertheless, these studies of tissue-specific degradation and biodistribution kinetics provide initial critical insights into the rate and extent of polymer degradation in tissues, which impacts drug release and biodistribution. Determination of nanoparticle degradation rate in tissues could greatly improve the design of drug delivery systems and lead to important insights about nanoparticle toxicity in general.

The pPDI of nanoparticles (presented as part of Supplementary Table 1 in the Supporting Information) shows trends that are relevant and understandable in conjunction with the biodistribution information. In the liver, there was a decrease in the pPDI over time for both nanoparticle sizes. It might be expected that the pPDI increases with time as more fragments in the chain are broken, thereby creating a wider distribution. However, the decrease in the pPDI over time can be explained by the fact that there is a loss of mass in the tissue over time indicating that degraded fractions, likely soluble oligomers, are being cleared from the liver, resulting in a total decrease in pPDI. The liver, a well-perfused organ, facilitates the dynamic exchange of material through the bloodstream. In the spleen, for the 200 nm nanoparticles, the pPDI decreased steadily most likely because the degraded fractions were cleared from the spleen. This assumption is supported by the fact that the biodistribution of 200 nm nanoparticles in the spleen decreased drastically after 3 h. For 500 nm nanoparticles in the spleen, the pPDI decreased steadily until the end of 1 week, starting 24 h after administration. In the biodistribution of 500 nm nanoparticles, there was a sudden decrease in the amount of nanoparticles in the spleen after 24 h, which includes the loss of degraded fractions. Therefore we see a decrease in the pPDI after 24 h. Furthermore, the amount of nanoparticles in the spleen is almost the same at 3 h and at 24 h, which is why we see the pPDI increase from 3 h to 24 h as a result of the degraded fraction present in the spleen by the end of 24 h. In the liver there is also an increase in the pPDI despite a mass loss. However, it should be noted that the mass loss in the liver from 3 h to 24 h is much less than what was observed in the liver for 200 nm particles and may indicate that a relatively large amount of loss is required over the first 24 h to yield reduced pPDI values.

3.4. Degradation Kinetics of PLGA Nanoparticles.

Several studies have shown that the hydrolytic degradation of poly lactic acid, poly glycolic acid, and their copolymer PLGA follows first-order kinetics.[22,23] The first-order degradation pattern can be represented by the following equation:

$$M = M_o(e^{-kt}) \quad (1)$$

where M is the molecular weight of the degrading polymer at time t, k is the rate constant of degradation, and M_o is the initial molecular weight of the polymer. Plotting Ln(M_w) against time for the *in vitro* degradation study gives the profiles depicted in Figure 7. The data, when fitted for linearity, give r^2 values of

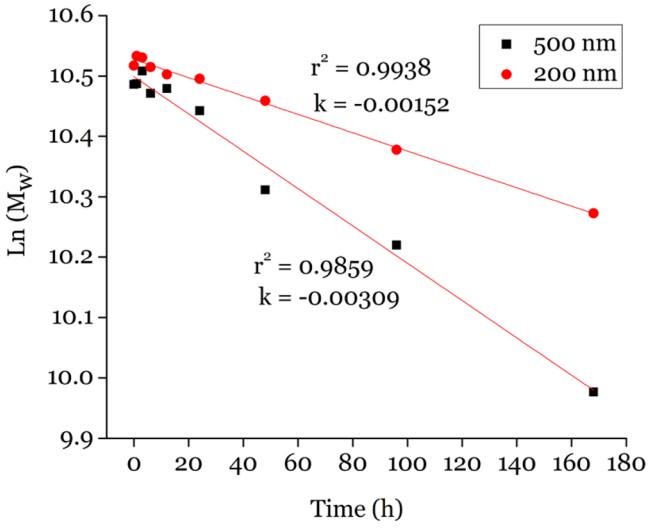

Figure 7. Ln(M_w) versus time for the *in vitro* degradation of 500 nm and 200 nm nanoparticles. The data were subjected to linear fit, and r^2 values confirm the linearity of the data.

0.9859 and 0.9938 for 500 nm and 200 nm nanoparticles, respectively. This indicates that the *in vitro* degradation of PLGA nanoparticles of both sizes follows first-order kinetics. The *in vitro* rate of degradation of 500 nm nanoparticles is 2 times faster than that of 200 nm nanoparticles (Figure 7).

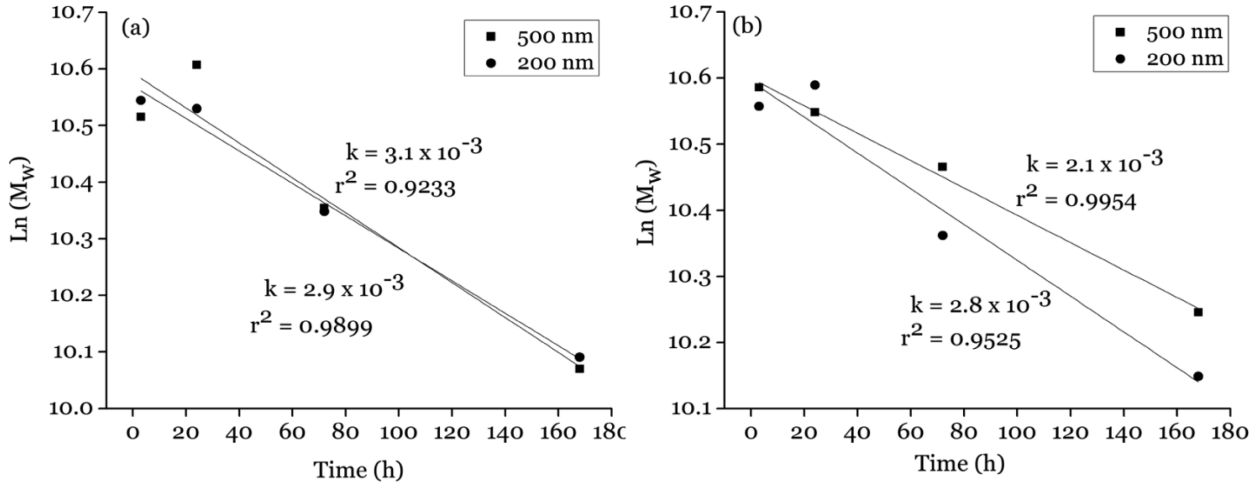

Figure 8. Ln(M_w) versus time for the *in vivo* degradation of 500 nm and 200 nm nanoparticles in (a) liver and (b) spleen. The data were subjected to linear fit, and r^2 values confirm the linearity of the data.

In the *in vivo* study, when the Ln(M_w) was plotted against time and the data were fitted for linearity (Figure 8), the r^2 values obtained suggest that the *in vivo* degradation in the liver and spleen also followed a first-order degradation pattern. For 500 nm nanoparticles in liver and spleen the r^2 values were 0.9233 and 0.9954, respectively. Similarly, for 200 nm nanoparticles in liver and spleen the r^2 values were 0.9899 and 0.9525, respectively. Important comparisons can be made for the degradation rates *in vivo* and *in vitro* for each nanoparticle size. The 500 nm nanoparticles in liver had a rate of degradation similar to that *in vitro*, whereas in spleen the degradation rate was 0.67 times that *in vitro*. On the other hand, the 200 nm nanoparticles in liver and spleen had a degradation rate nearly double that *in vitro* (Table 1). A discrepancy between *in vitro* and *in vivo* degradation exists for 200 nm particles, but does not exist for 500 nm particles. We theorize that this may be due to the autocatalytic degradation behavior described previously for PLGA where it is known that larger particles degrade quicker *in vitro*, as our results show, due to a reduced escape/diffusion of acidic degradation products compared to smaller counterparts of higher surface area.[10] We theorize that this degradation difference among the two particle sizes may be ameliorated *in vivo* where biological compartmentalization may hinder the local escape of acidic degradation products.

Table 1. First-Order Rate Constants of Degradation of Polymer Nanoparticles in Tissues and *in Vitro*[a]

	rate constant (k) ($\times 10^{-3}$)		
size (nm)	liver	spleen	*in vitro*
500	3.1 ± 0.2^{a}	$2.1 \pm 0.1^{a,b}$	$3.1 \pm 0.8^{b,c}$
200	2.9 ± 0.4^{d}	2.7 ± 0.4^{e}	$1.5 \pm 0.1^{c,d,e}$

[a]The rate constants were calculated by plotting Ln(M_w) versus time (t), and the data were fitted linearly, which then gives the slope (k) of the line for each data set. Superscript letters indicate statistical significance ($p < 0.05$) where values marked with "a" are significant from each other, values marked with "b" are significant from each other, and so on for each superscript letter.

The data on molecular weight and degradation kinetics together provide important insights into the pattern of nanoparticle degradation in tissues and help to establish the correlation between *in vivo* degradation and *in vitro* degradation. A clear *in vitro*–*in vivo* correlation cannot be directly made in a global sense, because in some cases the *in vitro* degradation rate is a good predictor and in others it is not. To our knowledge, this is the first such *in vivo* degradation study, and the potential of such work will be realized upon further investigation of additional nanoparticle sizes, physiochemical properties, and polymer chemistries.

The utility of measuring *in vivo* degradation will be of further interest when drug release kinetics can be correlated to degradation. Determining *in vivo* release kinetics will enable targeted drug treatments using nanoparticles to become more effective and efficient, but is not trivial and is a current research focus.

Although this method yielded much important information about the *in vivo* tissue degradation of polymeric nanoparticles, it has some limitations. The most important limitations are that a considerably large amount of formulation per tissue sample is needed to detect degradation in major tissues. In tissues that receive relatively low nanoparticle distribution, the degradation cannot be determined with the current detection modality. Additionally, for some polymers of low molecular weight (~10,000 Da or less) there could be significant interference in the chromatogram from the tissue signal, which will make it impossible to accurately separate the polymer signal and characterize it. Despite these technical limitations, this method still yields highly important information regarding quantitative biodistribution and biodegradation *in vivo*. We are currently focused on improving the method to overcome these technical limitations.

Knowledge of biodegradation coupled with that of biodistribution is necessary to design efficacious drug delivery systems, as it sheds light on the pharmacokinetics of the nanoparticle systems. Different organs have different nanoparticle deposition and degradation rates. Therefore, information regarding tissue deposition of the nanoparticles alone does not fully characterize the spectrum of nanoparticle pharmacokinetics. Since the nanoparticles degrade in tissues and are eliminated/excreted, knowing the biodegradation coupled with the biodistribution will give us a clearer understanding of the pharmacokinetics of degradable nanoparticle systems and the tissue pharmacokinetics of the drugs encapsulated by nano-

particles. All of this information will influence the design and safety considerations of polymeric drug delivery systems.

3.5. Conclusions. We have successfully shown the *in vivo* degradation of distributed PLGA nanoparticles in tissues at several time points after intravenous administration. We have also shown that differences exist between *in vitro* and *in vivo* degradation of PLGA nanoparticles. The smaller, 200 nm diameter nanoparticles had a faster degradation rate *in vivo* than *in vitro*. Conversely, compared to *in vitro* degradation, the larger, 500 nm diameter particles had a similar rate in the liver, but degraded more slowly in the spleen. For all particles there was a decrease in all the molecular weight parameters over time. Understanding *in vivo* biodegradation kinetics of polymer nanoparticles, in combination with biodistribution, will have major implications on drug delivery involving biodegradable polymer nanoparticles and microparticles. This method can be further improved and applied not only to PLGA-based delivery devices but to any degradable polymer used in biological systems.

■ ASSOCIATED CONTENT

Ⓢ Supporting Information

The full set of degradation data as well as representative chromatograms demonstrating degradation. This material is available free of charge via the Internet at http://pubs.acs.org.

■ AUTHOR INFORMATION

Corresponding Author

*E-mail: reineke@wayne.edu. Tel: 313-577-3761. Fax: 313-577-2033.

Notes

The authors declare no competing financial interest.

■ ACKNOWLEDGMENTS

This work was supported by the Department of Pharmaceutical Sciences, Eugene Applebaum College of Pharmacy and Health Sciences, and the Provost's Office, Wayne State University. We thank Professor David Oupicky at Wayne State University for giving us access to his laboratory equipment, in particular, the dynamic light scattering device, and Lisa Maroski for editing the manuscript.

■ REFERENCES

(1) Couvreur, P.; Vauthier, C. Nanotechnology: intelligent design to treat complex disease. *Pharm. Res.* **2006**, *23*, 1417−1450.

(2) Zolnik, B. S.; Burgess, D. J. Effect of acidic pH on PLGA microsphere degradation and release. *J. Controlled Release* **2007**, *122*, 338−344.

(3) Panyam, J.; Dali, M. M.; Sahoo, S. K.; Ma, W.; Chakravarthi, S. S.; Amidon, G. L.; Levy, R. J.; Labhasetwar, V. Polymer degradation and in vitro release of a model protein from poly(D,L-lactide-co-glycolide) nano- and microparticles. *J. Controlled Release* **2003**, *92*, 173−187.

(4) Wang, J.; Wang, B. M.; Schwendeman, S. P. Characterization of the initial burst release of a model peptide from poly(D,L-lactide-co-glycolide) microspheres. *J. Controlled Release* **2002**, *82*, 289−307.

(5) Danmark, S.; Finne-Wistrand, A.; Schander, K.; Hakkarainen, M.; Arvidson, K.; Mustafa, K.; Albertsson, A. C. In vitro and in vivo degradation profile of aliphatic polyesters subjected to electron beam sterilization. *Acta Biomater.* **2011**, *7*, 2035−2046.

(6) Pekarek, K. J.; Dyrud, M. J.; Ferrer, K.; Jong, Y. S.; Mathiowitz, E. In vitro and in vivo degradation of double-walled polymer microspheres. *J. Controlled Release* **1996**, *40*, 169−178.

(7) Shive, M. S.; Anderson, J. M. Biodegradation and biocompatibility of PLA and PLGA microspheres. *Adv. Drug Delivery Rev.* **1997**, *28*, 5−24.

(8) Cai, Q.; Shi, G.; Bei, J.; Wang, S. Enzymatic degradation behavior and mechanism of poly(lactide-co-glycolide) foams by trypsin. *Biomaterials* **2003**, *24*, 629−638.

(9) Pan, H.; Jiang, H.; Chen, W. The biodegradability of electrospun Dextran/PLGA scaffold in a fibroblast/macrophage co-culture. *Biomaterials* **2008**, *29*, 1583−1592.

(10) Dunne, M.; Corrigan, O. I.; Ramtoola, Z. Influence of particle size and dissolution conditions on the degradation properties of polylactide-co-glycolide particles. *Biomaterials* **2000**, *21*, 1659−1668.

(11) Li, M.; Al-Jamal, K. T.; Kostarelos, K.; Reineke, J. Physiologically based pharmacokinetic modeling of nanoparticles. *ACS Nano* **2010**, *4*, 6303−6317.

(12) Yallapu, M. M.; Gupta, B. K.; Jaggi, M.; Chauhan, S. C. Fabrication of curcumin encapsulated PLGA nanoparticles for improved therapeutic effects in metastatic cancer cells. *J. Colloid Interface Sci.* **2010**, *351*, 19−29.

(13) Mainardes, R. M.; Evangelista, R. C. PLGA nanoparticles containing praziquantel: effect of formulation variables on size distribution. *Int. J. Pharm.* **2005**, *290*, 137−144.

(14) Storm, G.; Belliot, S. O.; Daemen, T.; Lasic, D. D. Surface modification of nanoparticles to oppose uptake by the mononuclear phagocyte system. *Adv. Drug Delivery Rev.* **1995**, *17*, 31−48.

(15) Owens, D. E., 3rd; Peppas, N. A. Opsonization, biodistribution, and pharmacokinetics of polymeric nanoparticles. *Int. J. Pharm.* **2006**, *307*, 93−102.

(16) Albanese, A.; Tang, P. S.; Chan, W. C. The effect of nanoparticle size, shape, and surface chemistry on biological systems. *Annu. Rev. Biomed. Eng.* **2012**, *14*, 1−16.

(17) Florence, A. T.; Hillery, A. M.; Hussain, N.; Jani, P. U. Nanoparticles as carriers for oral peptide absorption: Studies on particle uptake and fate. *J. Controlled Release* **1995**, *36*, 39−46.

(18) Li, S. D.; Huang, L. Pharmacokinetics and biodistribution of nanoparticles. *Mol. Pharmaceutics* **2008**, *5*, 496−504.

(19) Korn, E. D.; Weisman, R. A. Phagocytosis of latex beads by Acanthamoeba. II. Electron microscopic study of the initial events. *J. Cell Biol.* **1967**, *34*, 219−227.

(20) Decuzzi, P.; Godin, B.; Tanaka, T.; Lee, S. Y.; Chiappini, C.; Liu, X.; Ferrari, M. Size and shape effects in the biodistribution of intravascularly injected particles. *J. Controlled Release* **2010**, *141*, 320−327.

(21) Markert, C. L.; Hunter, R. L. The distribution of esterases in mouse tissues. *J. Histochem. Cytochem.* **1959**, *7*, 42−49.

(22) Deng, M.; Chen, G.; Burkley, D.; Zhou, J.; Jamiolkowski, D.; Xu, Y.; Vetrecin, R. A study on in vitro degradation behavior of a poly(glycolide-co-L-lactide) monofilament. *Acta Biomater.* **2008**, *4*, 1382−1391.

(23) Farrar, D. F.; Gillson, R. K. Hydrolytic degradation of polyglyconate B: the relationship between degradation time, strength and molecular weight. *Biomaterials* **2002**, *23*, 3905−3912.